SPANDIDOS PUBLICATIONS

ONCOLOGY LETTERS 22: 620, 2021

Mammospheres of letrozole-resistant breast cancer cells enhance breast cancer aggressiveness

JANKIBEN R. PATEL[1*], KAREN M. GALLEGOS[1*], RASHIDRA R. WALKER[1], A. MICHAEL DAVIDSON[1], IAN DAVENPORT[2] and SYREETA L. TILGHMAN[1]

[1]Division of Basic Sciences, College of Pharmacy and Pharmaceutical Sciences, Florida A&M University, Tallahassee, FL 32307; [2]Division of Biological and Public Health Sciences, Department of Biology, College of Arts and Sciences, Xavier University of Louisiana, New Orleans, LA 70125, USA

Received January 30, 2020; Accepted May 11, 2021

DOI: 10.3892/ol.2021.12881

Abstract. Aromatase inhibitors (AIs), such as letrozole, are considered as first-line treatment for estrogen receptor-positive breast cancer in postmenopausal women. Despite the successful use of letrozole, resistance to therapy, tumor relapse and metastasis remain principal causes of patient mortality. Although there is no therapy currently available for AI-resistant breast cancer, previous reports have demonstrated that AI resistance is associated with hormone independence, increased growth factor signaling, enhanced cellular motility and epithelial to mesenchymal transition (EMT). This suggests a convergence of EMT and cancer stem cells (CSCs) in endocrine resistance. The present study evaluated the contribution of mammospheres in letrozole-resistant breast cancer by characterizing mammospheres and their potential impact on cellular motility. Ovariectomized immunocompromised female mice were inoculated in the mammary fat pad with either letrozole-resistant MCF-7 cells (LTLT-Ca) or letrozole-sensitive MCF-7 cells (AC-1). Subsequently, intratumoral CSC marker expression was assessed by immunohistochemistry. The results indicated that LTLT-Ca tumors were $CD44^+/CD24^+$, while AC-1 tumors presented low CD44/CD24 expression. Since mammosphere formation depends on CSCs, both cell lines were cultured either adherently (2D) or as mammospheres (3D) to assess the CD44/CD24 protein expression profile. When 3D culturing both cell lines, higher expression levels of CD44 and CD24 were observed when compared with their adherent counterparts, with the most robust change observed in the LTLT-Ca cell line. To quantitate the breast cancer stem cell activity, mammosphere formation assays were performed, and the LTLT-Ca cells formed mammospheres at a 3.4-fold higher index compared with AC-1 cells. Additionally, targeted gene expression arrays were conducted to compare the LTLT-Ca 3D and 2D cells, revealing that LTLT-Ca 3D cells displayed decreased expression levels of genes involved in cell adhesion and tumor suppression (e. g., E-cadherin, caveolin 1 and β-catenin). To validate this finding, wound healing assays were performed, and LTLT-Ca mammospheres exhibited a 70% wound closure, whereas AC-1 mammospheres exhibited a 39% wound closure. Collectively, the present findings demonstrated a strong association between AI-resistant mammospheres and an increased propensity for migration, which may be indicative of a poor prognosis.

Correspondence to: Dr Syreeta L. Tilghman, Division of Basic Sciences, College of Pharmacy and Pharmaceutical Sciences, Florida A&M University, 1415 S. Martin Luther King, Jr. Blvd., Tallahassee, FL 32307, USA
E-mail: syreeta.tilghman@famu.edu

[*]Contributed equally

Key words: letrozole resistance, breast cancer, cancer stem cells, epithelial to mesenchymal transition, aromatase inhibitors, mammospheres, CD44, CD24

Introduction

Although mortality rates for estrogen receptor-positive (ER^+) breast cancer in the US have been rapidly declining with the onset of successful endocrine therapy [i.e., aromatase inhibitors (AI) and selective estrogen receptor modulators], the development of resistance remains a lingering challenge. Previously, it has been demonstrated that AI resistance is associated with epithelial to mesenchymal transition (EMT), increased growth factor signaling, and enhanced motility (1-7). In cancer, EMT refers to several phenotypic changes, with epithelial cells transitioning into a mesenchymal phenotype (8). The resultant phenotype reveals increased migration and invasiveness, loss of polarity, and resistance to apoptosis (9). Furthermore, the emergence of a subpopulation of radiation- and chemo-resistant breast CSCs within AI-resistant breast tumors (1) continues to complicate therapeutic interventions.

In tumors, CSCs dictate invasion, metastasis, and drug resistance (10). Previous reports have revealed that these highly tumorigenic CSCs are involved in relapse, metastasis, and EMT (11). CSCs are characterized by their preferential ability to initiate and propagate tumor growth and their selective capacity for self-renewal and differentiation (12). Reportedly, Al-Hajj *et al* (13) were the first to definitively identify and characterize human breast CSCs from patients. They have

demonstrated that human breast cancers contain a subpopulation of $CD44^{high}/CD24^{low}$ cells that exhibit stem cell and malignant properties. Several reports have revealed that CSCs are enriched among circulating tumors in the peripheral blood of patients with breast cancer (14). Recent studies have shown that EMT, an early step of tumor migration, can differentiate cancer cells into a CSC-like state (15) thereby establishing a functional link between CSCs and EMT. Currently, effective targeted approaches to endocrine-resistant breast cancer are lacking owing to an inability to inhibit breast CSCs and completely unravel the rate-limiting proteins and pathways that drive metastatic disease.

The mammosphere formation assay was established based on the spheroid model (16). Mammospheres represent a pre-cancerous state and also act as a surrogate indicator for the presence of CSCs (17). This model is utilized based on the rationale that only epithelial cells can survive in mammosphere suspension cultures, whereas other cells undergo apoptosis owing to the higher self-renewal capacity of stem cells when compared with other cells (18-20). Considering the advantages and appropriateness of this model, we evaluated the characteristics of letrozole-resistant mammospheres and their implication toward a more aggressive and migratory phenotype.

Materials and methods

Cell culture. Generation of the LTLT-Ca cell line (long-term letrozole treated MCF-7 cells stably transfected with the human aromatase gene) was previously described (4). Briefly, LTLT-Ca cells were isolated from tumors of aromatase-transfected MCF-7 cells grown in ovariectomized BALB/c athymic mice after 56 weeks of letrozole treatment. The tumors start proliferating in the presence of the drug after long-term treatment. Human LTLT-Ca cells were generously provided by Dr Angela Brodie and were cultured in 75-cm^2 flasks in phenol red-free IMEM (Improved Minimum Essential Medium; Invitrogen; Thermo Fisher Scientific, Inc.), supplemented with 10% charcoal-dextran-stripped fetal bovine serum (FBS), 100 U/ml penicillin (Gibco; Thermo Fisher Scientific, Inc.), 100 U/ml streptomycin (Gibco; Thermo Fisher Scientific, Inc.), 25 μg/ml amphotericin B (Gibco; Thermo Fisher Scientific, Inc.), 7.5 μg/ml geneticin (Invitrogen; Thermo Fisher Scientific, Inc.) 1 μM letrozole (Sigma-Aldrich; Merck KGaA). The culture flasks were maintained in a humidified atmosphere of 5% CO_2 at 37˚C. Letrozole-sensitive AC-1 cells were maintained in DMEM (Dulbecco's modified Eagle's medium; Invitrogen; Thermo Fisher Scientific, Inc.), supplemented with 5% FBS, 100 U/ml penicillin (Gibco; Thermo Fisher Scientific, Inc.), 100 U/ml streptomycin (Gibco; Thermo Fisher Scientific, Inc.), 25 μg/ml amphotericin B (Gibco; Thermo Fisher Scientific, Inc.), 7.5 μg/ml geneticin (Invitrogen; Thermo Fisher Scientific, Inc.) in a humidified atmosphere of 5% CO_2 at 37˚C. T47D letrozole-sensitive (T47Darom) and T47D letrozole-resistant (T47DaromlR) cells were cultured as previously described by Gupta *et al* (21) and were a generous gift from IIT Research Institute. Mycoplasma testing was performed for all cell lines. All cells were authenticated by short tandem repeat (STR) profiling by American Type Culture Collection (ATCC), confirming that the AC-1 and LTLT-Ca cell lines shared more than 85% homology with the MCF-7 cell lines, while the T47Darom and T47DaromLR cell lines shared more than 85% homology with the T47D cell line. Cell lines with 80% match are considered related (derived from a common ancestry). In brief, 17 STR loci plus the sex-determining locus, amelogenin, were amplified using the commercially available PowerPlex® 18D Kit (Promega). The cell line samples were processed using the ABI Prism® 3500 xL Genetic Analyzer. Data were analyzed using the GeneMapper® ID-X v1.2 software (Applied Biosystems). Appropriate positive controls (MCF-7 or T47D cell lines) were run and confirmed for each sample submitted. Cell lines were authenticated using STR analysis as described in 2012 in the ANSI Standard (ASN-0002) by the ATCC Standards Development Organization (SDO), as well as Capes-Davis *et al* (22).

Mammosphere culture and mammosphere formation assay. AC-1 and LTLT-Ca cells were grown in regular media to attain 80-90% confluency, and after media was removed, cells were rinsed twice with Hank's Balanced Salt Solution (HBSS; StemCell Technologies, Vancouver, Canada) to remove residual culture media. Then, cells were gently scraped and resuspended in 10 ml of MammoCult™ media (StemCell Technologies). Next, cells were centrifuged at 500 x g for 3 min at room temperature. The supernatant was aspirated, and the pellet was resuspended into a single cell suspension in 2 ml of MammoCult™ media. Cell viability and concentration were determined by the Trypan Blue exclusion assay. For mammosphere cultures, the seeding density for both cell lines were 100,000 cells per 25-cm^2 suspension flasks (CellTreat Scientific Products). All flasks were incubated in a 5% CO_2 humidified incubator at 37˚C for at least 7 days. Once mammospheres were detected by light microscopy, the cells were harvested as detailed below in western blot analysis.

Mammosphere self-renewal assay. For primary mammosphere formation, AC-1 and LTLT-Ca cells were enumerated, and 20,000 cells/well were seeded in ultra-low adhesion 6-well plates. The cultures were incubated in a 5% CO_2 humidified incubator at 37˚C for 7 days and spheres ≥60 μm were counted and recorded. After primary spheres were formed, secondary mammosphere formation was conducted for both AC-1 and LTLT-Ca cells by dissociating the primary spheres with Accutase (Sigma-Aldrich; Merck KGaA) according to the manufacturer's instructions. Next, 20,000 cells/well were seeded in ultra-low adhesion 6-well plates, with the remainder of the assay conducted as described for primary mammosphere formation.

Cell proliferation assay. Proliferation assays were conducted as previously described (23). Briefly, AC-1 or LTLT-Ca cells were seeded in 96-well plates at a density of 1 x 10^3 cells/well in a total volume of 100 μl and allowed to attach overnight. Background levels were determined by preparing blank samples, with media added to wells in the absence of cells. On the following day, 10 μl of resazurin dye (Sigma-Aldrich; Merck KGaA) was added to each well and incubated for 4 h at 5% CO_2 and 37˚C. Samples were agitated for 1 min and the fluorescence was measured at 24, 48, 72, 96 and 120 h using a Biotek Synergy H1 microplate reader (BioTek

Instruments, Inc.) to measure fluorescence intensity at 550 nm excitation/590 nm emission background wavelengths. All experiments were performed with n≥3 and a total of 3 biological replicates were performed. The proliferative activity was determined and calculated as described below: Proliferative activity = [Fluorescence of viable cells-Fluorescence of blank (media only)].

Wound healing assay. AC-1 and LTLT-Ca mammospheres were dissociated and single cells were seeded at a density of $1.5x10^5$ cells/well in 6-well tissue culture plates until 100% confluency was attained. A scratch (wound) was made down the center of each well using a 10 μl pipette tip, and new media was added. Each scratch was immediately imaged (at 0 h) 3 times at different points using the 5X objective on a Zeiss AX10 fluorescence microscope. Images were captured using Olympus CellSens Standard 1.16 software. Then, cells were grown at 37˚C, 5% CO_2, and images were captured at 24 and 48 h. The wounds were measured and analyzed using the WimScratch Wound healing Software.

Gel electrophoresis and western blot analysis. Briefly, adherent cells were gently scraped and homogenized in cold RIPA buffer supplemented with 2X protease and phosphatase inhibitors (Thermo Fisher Scientific, Inc.). Mammospheres were centrifuged at 400 x g for 7 min at 4˚C and then resuspended in cold RIPA buffer. All samples were incubated for 30 min on ice and then centrifuged for 20 min at 12,000 rpm. The protein extract was quantified in each sample using the Bradford assay. For gel electrophoresis, all samples were incubated with Laemmli protein sample buffer (Bio-Rad) at 70˚C for 10 min. Then, 75 μg of denatured protein was separated using 4-20% Mini-PROTEAN® TGX™ Precast Protein Gels (Bio-Rad) and transferred to polyvinylidene difluoride (PVDF) membranes. All blots were blocked for 1 h with 5% bovine serum albumin (BSA) in phosphate-buffered saline (PBS) and 0.1% Tween-20 (PBS-T) buffer. Following incubation with primary antibodies, anti-CD24 antibody at 1:1,000 dilution (catalog no. ab179821; Abcam) and anti-CD44 antibody 1:1,000 dilution (catalog no. ab157107; Abcam), the membranes were incubated with the anti-rabbit secondary antibody (catalog no. 7074S; Cell Signaling Technology). The protein bands were detected using the Clarity Max Western ECL Substrate (Bio-Rad) according to the manufacturer's instructions. Immunoreactive bands were visualized using the ChemiDoc XRS imaging system (Bio-Rad). The exposure time was automatically detected by the imaging system. The protein bands were analyzed using Image Lab software (Bio-Rad). Arbitrary densitometry units were quantified and expressed as mean ± standard deviation. The bands were normalized to the housekeeping protein bands (GAPDH), whereby the density of the target protein in each lane was multiplied by the ratio of the loading control density from the control sample (lane 1) to the loading control density of other lanes. The immunoblot images are representative of more than three independent experiments with a minimum of 2 duplicates per sample.

Animal letrozole- sensitive and letrozole-resistant cell tumors. SCID female ovariectomized mice (29-32 days old) were obtained from Charles River Laboratories. All animals underwent an adaptation period of 5-7 days in a pathogen-free and sterile environment, with a phytoestrogen-free diet. AC-1 and LTLT-Ca cells in the exponential phase of growth were harvested using PBS supplemented with 2% EDTA solution and washed. Viable cells ($5x10^6$) in a 50 μl sterile PBS suspension were mixed with 100 μl Matrigel Reduced Factors (BD Biosciences). AC-1 and LTLT-Ca cells were injected into the mammary fat pad (n=5 for each group). For AC-1 cells, estrogen pellets (0.72 mg, 60-day release; Innovative Research of America) were subcutaneously implanted in the lateral area of the neck, in the middle point between the ear and shoulder, using a precision trocar (10 gauge). All animal procedures were performed under anesthesia using a ketamine/xylazine mixture consisting of 80 mg/kg of ketamine and 10 mg/kg of xylazine. Tumors were allowed to form over 10 days. Tumor volume was measured weekly for 8 weeks using a digital caliper. Tumor volume was calculated using the following formula: $4/3LM^2$, where L is the larger radius and M is the smaller radius. At necropsy, animals were euthanized by exposure to a CO_2 chamber with a flow rate of 2L of CO_2/min at a displacement rate of 30-70% of the chamber volume per minute. Death was confirmed by evidence of pale eyes and the absence of a heartbeat and lack of respiration for at least 1 min. For further analysis, tumors were removed and fixed in 10% formalin. All procedures involving animals were conducted in compliance with state and federal laws, standards of the US Department of Health and Human Services, and guidelines established by the Xavier University of Louisiana University Animal Care and Use Committee. The facilities and laboratory animal program of Xavier University of Louisiana are accredited by the Association for the Assessment and Accreditation of Laboratory Animal Care.

Immunohistochemistry of letrozole- sensitive and letrozole-resistant tumors. For immunohistochemical analysis, AC-1 and LTLT-Ca tumors were grown as described above, using groups of 5 animals, each containing 2 tumors. Immunohistochemistry was performed as previously described (24). Briefly, a minimum of one tumor tissue per animal (n=5/group) was fixed, deparaffinized, and rehydrated. Anti-CD24 (catalog no. MAB5248, 1:100 dilution; R&D Systems) and anti-CD44 (catalog number MAB7045, 1:100 dilution; R&D Systems) antibodies were used as potential markers. Staining was performed using EXPOSE mouse and rabbit specific HRP/DAB detection IHC kit (catalog number: ab80436; Abcam). Cells were counterstained with hematoxylin for 3 min, dehydrated, and mounted. Once slides were prepared, at least 4 microscopic fields were randomly selected for each tumor and visualized using x20 magnification. Data are presented as a semi-quantitative Histo-score, where the fractions were assigned as negative (score 0), weakly positive (score 1), positive (score 2), or strongly positive (score 3). All slides were scored blindly by three individual investigators.

Immunofluorescence of letrozole- sensitive and letrozole-resistant cells. Immunofluorescence was performed as previously described (24). Briefly, three replicates of LTLT-Ca cells were seeded in 8-well chamber slides (Thermo Fisher Scientific, Inc.) pre-coated with 2% gelatin and grown to

50% confluence. Cells were fixed with formaldehyde, permeabilized with 0.5% NP-40 in PBS, and rinsed with PBS. The slides were blocked with 10% goat serum (Invitrogen; Thermo Fisher Scientific, Inc.) in PBS and incubated with anti-CD24 (1:200) catalog no. sc-19585, anti-HCAM (1:200) catalog no. sc-7927, and anti-Ki67 (1:200) catalog no. sc-23900, (Santa Cruz Biotechnology Inc.). Then, samples were washed with 1% goat serum in PBS and incubated with Alexa Fluor goat anti-rabbit-488 (1:1,000), catalog number: A-11008, or Alexa Fluor goat anti-mouse-488 secondary antibodies (1:1,000), catalog number: A-11001 (Invitrogen; Thermo Fisher Scientific, Inc.) in 10% goat serum. The samples were washed and stained with 300 nM DAPI (Invitrogen; Thermo Fisher Scientific, Inc.). The slides were imaged using an Olympus Bx41 microscope (Olympus) and captured using DP72 CCD driven by DP2 software (Olympus); the color images were combined using ImageJ software.

Reverse transcription-quantitative PCR (RT-qPCR) for 2D vs. 3D letrozole-resistant cells. Briefly, LTLT-Ca cells were cultured adherently in 75-cm^2 flasks in phenol red-free IMEM supplemented with 5% charcoal-stripped-FBS or as mammospheres as described above, cultured until 70%–80% confluency. Total RNA was extracted from cells using RNeasy (Qiagen) following the manufacturer's recommendations. Each array profiles the expression of a panel of 84 genes including 7 internal controls and 5 housekeeping gene controls. For each array, 2 μg of RNA was reverse-transcribed into cDNA in the presence of gene-specific oligonucleotide primers using the iScript cDNA Synthesis kit (Bio-Rad) as described in the manufacturer's protocol. The cDNA template was mixed with the appropriate ready-to-use PCR master mix (Bio-Rad). Equal volumes were measured (in aliquots) into each well of the same plate, and then the real-time PCR cycling program was run as described previously (7). RT-qPCR was performed using the manufacturer's protocols for Human Cell Motility (PAHS-128ZD) and Human Epithelial to Mesenchymal Transition (PAHS-090ZD) (EMT) RT^2 Profiler PCR Array (Qiagen). Relative gene expression was calculated using the $2^{-\Delta\Delta Cq}$ method (25), in which Ct indicates the fractional cycle number where the fluorescent signal reaches the detection threshold. The 'delta-delta' method uses the normalized ΔCt value of each sample, calculated using a total of five housekeeping gene control genes (18S rRNA, HPRT1, RPL13A, GAPDH and ACTB) (26). Fold change values are presented as average fold change = $2^{-(\text{average } \Delta\Delta Ct)}$ for genes in treated samples, relative to control samples. Differences in gene expression between groups were calculated using Student's t-test, in which fold changes ≤3 were considered significant. All experiments were performed with a minimum of three biological replicates.

Statistical analysis. Studies involving more than 2 groups were analyzed by 1-way ANOVA with Tukey's posttest analysis; all others were subjected to unpaired Student's t test and are summarized as the mean ± standard error of the mean (SEM) using Graph Pad Prism V.6 (GraphPad Software, Inc.). Data are expressed as the mean unit ± SEM ($^{****}P<0.0001$, $^{***}P<0.001$, $^{**}P<0.01$, $^{*}P<0.05$).

Results

Increased presence of cancer stem cell markers is associated with letrozole resistance. We have previously demonstrated that as breast cancer cells transition from letrozole-sensitive to letrozole-resistant, they are associated with estrogen independence, enhanced cellular motility, and an EMT-like phenotype (7,24). EMT is linked to the progression of cancer, as well as increased stemness of tumors (27). To examine the expression of two putative breast CSC markers in letrozole-sensitive (AC-1 cells) and letrozole-resistant (LTLT-Ca cells) breast cancer cell lines, we performed immunoblotting analysis. Considering that the mammosphere formation assay is employed as a surrogate reporter of cancer stem cell activity, both cell lines were cultured either adherently (2D) or in suspension (3D) as mammospheres. Our results demonstrated that when both AC-1 and LTLT-Ca cells were cultured as mammospheres, higher levels of CD24 and CD44 were expressed when compared with their adherently cultured counterparts (Fig. 1). On comparing CD24 expression between 2D and 3D cells, AC-1 3D cells exhibited an increase in CD24 expression exceeding 25%, while LTLT-Ca 3D cells exhibited a 500% increase in CD24 expression when compared with their 2D counterparts. When CD44 expression was examined, AC-1 3D and LTLT-Ca 3D cells exhibited increased CD44 expression (75 and 50%, respectively), suggesting that in both cell lines, mammosphere cultures presented enriched CSC characteristics when compared with cells cultured adherently, irrespective of their response to letrozole. Furthermore, a similar result was observed in T47D letrozole-sensitive and letrozole-resistant cell lines (Fig. S1).

Although *in vitro* human breast cancer cell models are useful screening tools, they can be limited by the absence of the breast tumor microenvironment. As *in vitro* cultured cells exhibit less complexity when compared with those *in vivo*, AC-1 and LTLT-Ca cells were inoculated into nude mice and allowed to form tumors (Fig. S2). The maximum diameter and volume of the AC-1 tumors were 6.36 x 6.78 mm and 365.66 mm^3 respectively, while the maximum diameter and volume of the LTLT-Ca tumors were 5.24 x5.85 mm and 214.17 mm^3 respectively. Then, tumors were excised, and CD24 and CD44 protein expressions were examined by immunohistochemistry. In addition, hematoxylin-eosin staining was performed. Letrozole-sensitive tumors revealed markedly less CD44 expression when compared with letrozole-resistant tumors, scoring 1 and 3, respectively (Fig. 2), whereas CD24 expression was higher in letrozole-resistant tumors than in letrozole-sensitive tumors, scoring 2 and 1, respectively (Fig. 2). In summary, the expression of CSC markers in tumors was $CD44^+/CD24^+$ in letrozole-resistant cells (LTLT-Ca) and low CD44/CD24 in letrozole-sensitive cells (AC-1 cells); meaning that LTLT-Ca tumors had higher expression of both CD44 and CD24 and AC-1 tumors had low expression of CD44 and CD24.

Letrozole resistance is associated with increased stemness. As marked differences were observed in the CD44/CD24 expression profile between AI-sensitive and AI-resistant tumors, we examined whether these differences correlated with the self-renewal capacity by using the mammosphere

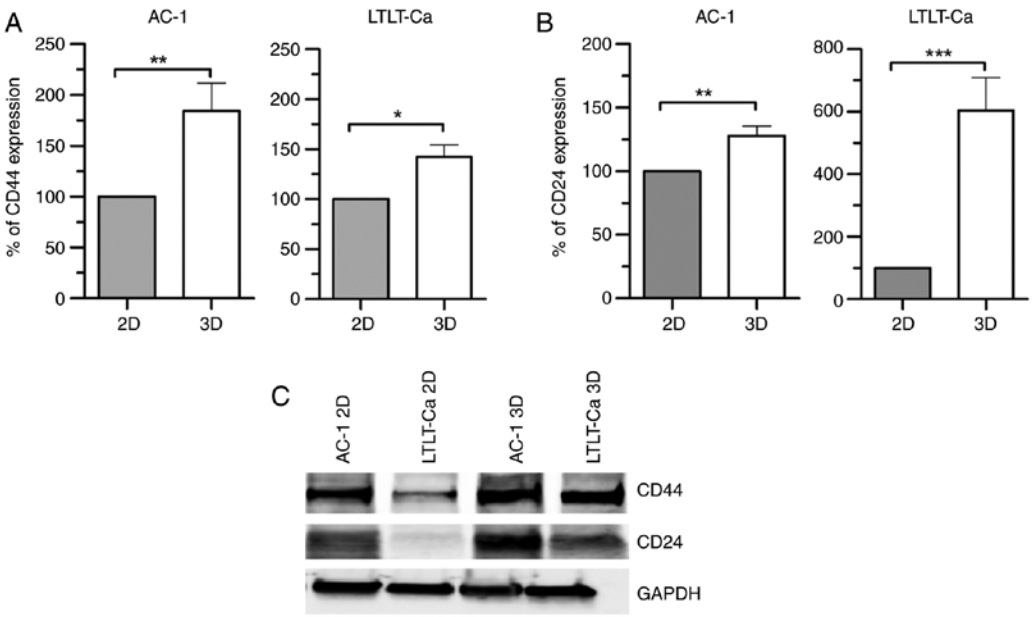

Figure 1. (A) CD44 and (B) CD24 expression in letrozole-sensitive (AC-1) and letrozole-resistant (LTLT-Ca) breast cancer cells cultured adherently (2D) or as mammospheres (3D). All cells were assayed by immunoblotting to examine the expression levels of CD44, CD24 and GAPDH (loading control). (C) Representative immunoblot showing the protein expression levels of CD44, CD24 and GAPDH. Graphs depict normalized percentages of protein expression relative to 2D cell counterparts. The immunoblot images are representative of more than three independent experiments with a minimum of two duplicates per sample. Comparison of 2D vs. 3D treatments was analyzed by an unpaired Student's t-test using GraphPad Prism software. $^{***}P<0.0004$, $^{**}P<0.0024$, $^{*}P\leq0.038$.

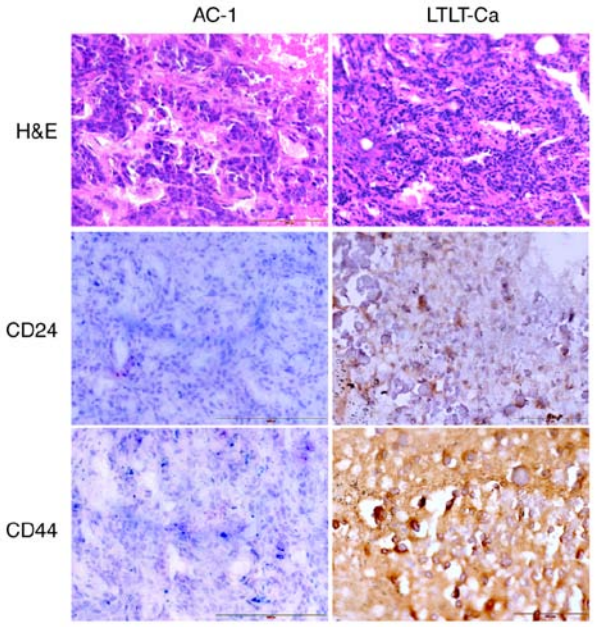

Figure 2. Immunohistochemical analysis of letrozole-sensitive (AC-1) and letrozole-resistant (LTLT-Ca) tumors. Representative sections of tumors were stained with H&E, anti-CD24 and anti-CD44 antibodies. The left panels present AC-1 tumor sections, and the right panels present LTLT-Ca tumor sections. Original magnification, x40. Scale bar, 100 μm.

self-renewal assay. AC-1 and LTLT-Ca cells were seeded at a low density in an environment that prevented adherence, thus enabling proliferation in suspension as spherical clusters (28). Interestingly, LTLT-Ca cells formed mammospheres at a 3.4-fold higher index when compared with AC-1 cell mammospheres (Fig. 3A). Culture images were obtained to examine their morphology, demonstrating that letrozole-resistant cells formed hollow mammospheres, while letrozole sensitivity was associated with solid mammospheres (Fig. 3B). Both cell lines formed symmetrical and tightly packed mammospheres. The mammospheres underwent a second passage, and LTLT-Ca mammospheres showed a 2.9-fold increase in mammosphere formation when compared with AC-1 cells. Compared with primary mammospheres, the total number of secondary mammospheres decreased; however, the ratio of secondary mammosphere formation between AC-1 and the LTLT-Ca mammospheres was similar to the primary mammosphere formation ratio. Based on this assay, letrozole-resistant cells were more highly associated with increased self-renewal capacity when compared with letrozole-sensitive cells. To determine whether the increase in LTLT-Ca mammosphere formation could be attributed to enhanced cell growth, proliferation assays were performed to compare both cell lines. AC-1 cells demonstrated a greater proliferative capacity than LTLT-Ca cells, suggesting that the increase in LTLT-Ca mammosphere formation was independent of cell proliferation (Fig. 4). To complement this finding, immunofluorescent analysis of LTLT-Ca mammospheres was conducted, and the LTLT-Ca mammospheres were $CD44^{+}$/CD24 (Fig. S3), similar to the tumors and adherent cultures. Furthermore, LTLT-Ca mammospheres stained positive for Ki67, a common cell proliferation marker, indicating their proliferative capacity.

Letrozole-resistant mammary cancer stem cells promote an invasive phenotype. As previous reports have confirmed that LTLT-Ca cells demonstrate greater migratory ability than AC-1 cells (7), we measured the expression of genes involved in motility and EMT, to assess whether the presence of CSCs was associated with a migratory phenotype. Accordingly, LTLT-Ca cells were cultured either adherently or as mammospheres, with targeted gene expression arrays

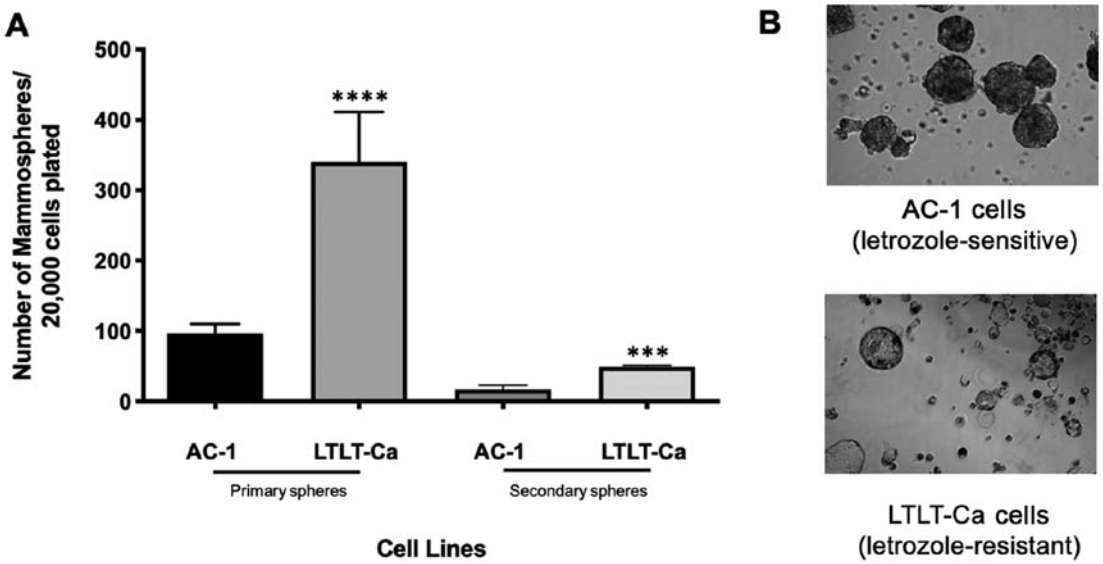

Figure 3. Mammosphere formation assays. AC-1 and LTLT-Ca cells were grown as primary and secondary mammospheres (3D), and (A) the total number of mammospheres was counted and plotted. Error bars indicate the SEM, n=4 independent cell samples/group. ****P<0.0001, ***P<0.001 vs. AC-1. (B) Representative images of primary mammospheres for each cell line. Original magnification, x10.

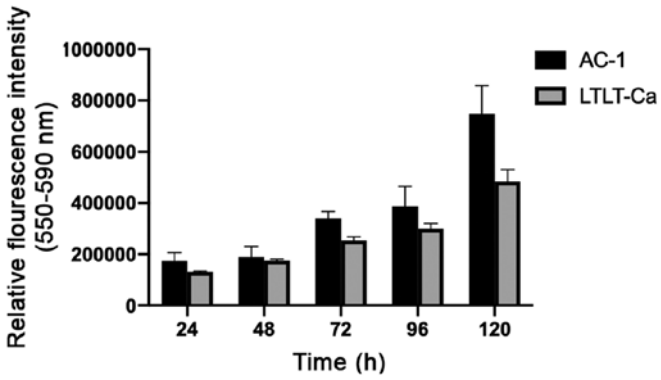

Figure 4. Letrozole-sensitive and letrozole-resistant breast cancer cell proliferation assay. Both AC-1 and LTLT-Ca cells were cultured, and cellular proliferation was measured using the resazurin assay. The graph indicates the proliferation (absorbance) after 24, 48, 72, 96 and 120 h. Results are presented as the mean unit ± SEM of three independent experiments performed in triplicate.

were conducted to measure the expression of genes involved in cellular motility and EMT (genes that were significantly altered where P<0.05 are shown in Table I). When compared with LTLT-Ca adherent cells, LTLT-Ca mammospheres displayed a -12.01-fold, -6.44-fold, and -8.14-fold decrease in the expression of caveolin-1, E-cadherin, and β-catenin, respectively. Interestingly, LTLT-Ca mammospheres exhibited a -3.33-fold and -3.29-fold decrease in epidermal growth factor receptor (EGFR) and integrin αV (CD51) expression. In addition to genes involved in motility, we also observed increased expression of TFPI-2 (4.42-fold) and STEAP1 (3.17-fold).

As proof of concept, a scratch assay (i.e., wound healing assay) was performed to assess whether the letrozole-resistant mammospheres impacted migratory behavior (Fig. 5). The results demonstrated that as early as 24 h, the letrozole-resistant mammospheres began migrating faster than the letrozole-sensitive mammospheres (Fig. 5). After 48 h, this effect was even more pronounced, and the LTLT-Ca cell wound closure was 70%, whereas the AC-1 wound closure was 39%, suggesting that as cells acquire resistance and express putative breast CSC markers, they become more aggressive through increased motility. Taken together, as letrozole-resistant cells acquire CSC characteristics, they are less associated with epithelial-like features, progressing toward a more mesenchymal phenotype.

Discussion

Letrozole resistance remains a major clinical obstacle. Although newer targeted therapeutic approaches that combine letrozole and palbociclib (a CDK4/6 inhibitor) are available, this therapeutic strategy has been reserved for ER-positive metastatic breast cancer patients. Unfortunately, there are no effective targeted therapies currently available for ER-negative, letrozole-resistant metastatic breast cancer patients. Therefore, identifying mechanisms of resistance among this population is highly significant. Previously, Al-Hajj *et al* (13) have demonstrated that $CD44^+/CD24^-$/low cells within a breast tumor possess self-renewal properties and are capable of tumor formation. Therefore, it is crucial to understand this cell subpopulation, as they are associated with cancer recurrence and treatment resistance. Thus, these cells must be targeted for eradication to prevent tumor relapse. To comprehensively understand the role of mammospheres in breast cancer resistance, we performed a series of studies to characterize CSC markers in letrozole-resistant breast cancer cells. Although CD44 is considered the most established CSC marker in a majority of cancers (29), CD24 remains controversial owing to its prognostic value and significance (30).

Immunoblots were performed and revealed a marked difference in the CD44 and CD24 expression profiles between adherent cells and mammospheres of cells, as well as between letrozole-resistant vs. letrozole-sensitive tumors. Letrozole- resistant mammospheres demonstrated a higher expression of both CD44 and CD24 than adherent cells. Our

Table I. SuperArray analysis of gene expression altered by letrozole-resistant mammospheres.

Gene symbol	Gene description	Fold change (LTLT-Ca mammospheres/ LTLT-Ca adherent cells)	Gene aliases
CAV1	Caveolin 1	-12.01	BSCL3, CGL3, MSTP085, VIP21
CAV2	Caveolin 2	-3.33	CAV, MGC12294
CDH1	E-cadherin	-6.44	Arc-1, CD324, CDHE, ECAD, LCAM, UVO
CTNNB1	Catenin (cadherin-associated protein), β1	-8.14	CTNNB, DKFZp686D02253, FLJ25606, FLJ37923
EGFR	Epidermal growth factor receptor	-3.33	ERBB, ERBB1, HER1, PIG61, mENA
F11R	F 11 Receptor	-6.40	CD321, JAM, JAM1, JAMA, JCAM, KAT, PAM-1
ITGAV	Integrin, αV	-3.29	CD51, DKFZp686A08142, MSK8, VNRA
KRT19	Keratin 19	-4.07	CK19, K19, K1CS, MGC15366
MET	Met proto-oncogene	-5.38	AUTS9, HGFR, RCCP2, c-Met
PTK2	PTK2 protein tyrosine kinase 2	-3.05	FADK, FAK, FAK1, FRNK, pp125FAK
STEAP1	Six transmembrane epithelial antigen of the prostate 1	3.17	MGC19484, PRSS24, STEAP
TFPI2	Tissue factor pathway inhibitor 2	4.42	FLJ21164, PP5, REF1, TFPI-2
TGFB2	Transforming growth factor, β2	-4.23	MGC116892, TGF-β2

Basal gene expression levels of LTLT-Ca cells cultured adherently vs. LTLT-Ca cells cultured in suspension were examined. Changes ± 3-fold are shown.

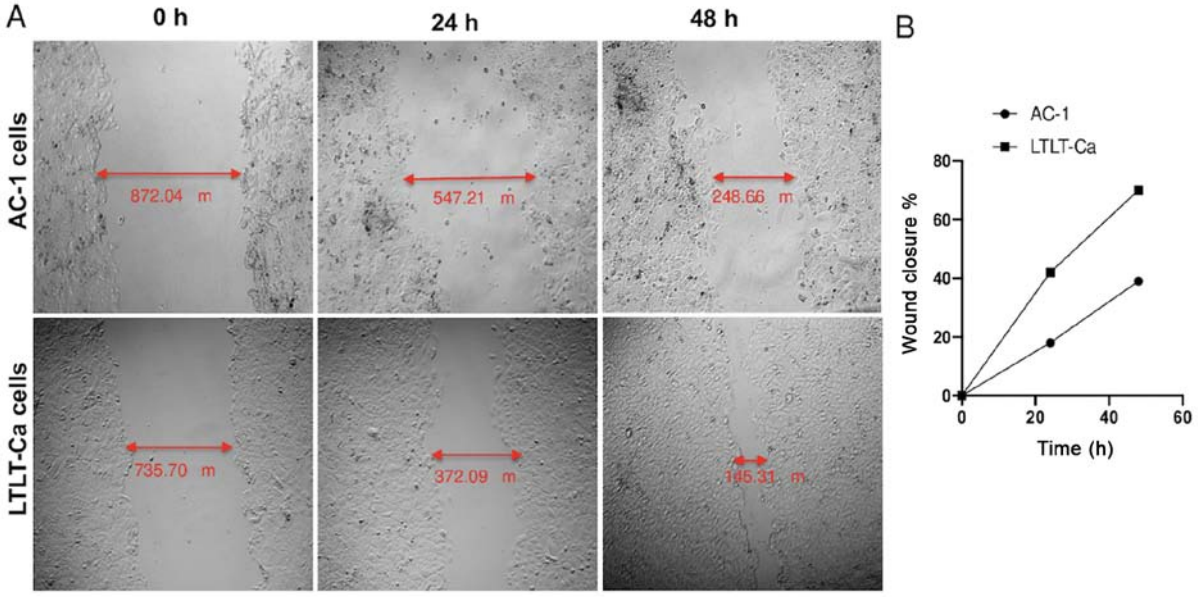

Figure 5. Letrozole-resistant mammospheres are highly migratory. (A) AC-1 and LTLT-Ca mammosphere migration was detected using a wound healing assay. The wound distance was measured after 0, 24 and 48 h. Original magnification, x5. (B) Graphical representation of the percentage of wound closure.

in vitro findings are in accordance with previous studies reporting high CD44 expression in half of the breast cancer cell lines studied and that most of the cell lines expressed increased amounts of CD24 (30). Some results obtained by Ricardo *et al* (30) were also corroborated by Li *et al* (31,32), where it was suggested that the CD44/CD24 ratio would serve as a more effective marker to identify stemness of cancer cells. Our letrozole-resistant tumors were $CD44^+/CD24^+$, while the letrozole-sensitive tumors had low levels of CD44/CD24. To further analyze the LTLT-Ca mammospheres, immunofluorescent staining was performed, and results were consistent with the immunoblots. Although we expected that LTLT-Ca tumors would exhibit reduced CD24 expression, our findings were substantiated by previous reports demonstrating

that the MDA-MB 468 triple-negative breast cancer cell line exhibits a similar $CD44^+/CD24^+$ expression profile (30). This phenotype is indicative of a highly differentiated basal/epithelial cell type. In this study, our results regarding the $CD44^+/CD24^+$ phenotype may indicate interconversion between phenotypes. Furthermore, our findings suggest that the epithelial-like $CD44^+/CD24^+$ phenotype can readily give rise to $CD44^+/CD24^-$ cells during tumor initiation (33). The $CD44^+/CD24^+$ phenotype may represent a transient state as cells progress to a more mesenchymal $CD44^+/CD24^-$ state.

An additional consideration is that as tumors were formed, the mice may be affected by other factors, including the tumor microenvironment and the potential contribution of mouse stem cells. The former plays a major role in cellular signaling, cell-cell communication, and cell surface markers such as CD24 and CD44, which exhibit variable expression levels at different stages of tumorigenesis. Since mouse specific stem cell markers were not explicitly examined, this may represent another avenue contributing to tumor formation and a limitation to this present study.

One of the most striking morphological features observed was that LTLT-Ca cells formed hollow mammospheres, whereas AC-1 cells formed solid mammospheres. Although still unclear, this change in morphology is likely associated with changes that occur as cells transition from a letrozole-sensitive to a letrozole-resistant phenotype. Previous reports from our research group have revealed that compared with letrozole-sensitive AC-1 cells, LTLT-Ca cells exhibit a change in cell morphology from a rounded, uniform cell body to a less organized cell body with protrusions indicative of EMT (7). The mammosphere formation assay revealed that LTLT-Ca cells were able to form more mammospheres than AC-1 cells in both primary and secondary passages independent of proliferation.

Considering these morphological alterations along with the increased mammospheres formation potential of LTLT-Ca cells, we aimed to clarify whether mammosphere culture conditions revealed novel changes in motility and gene expression that are absent in adherent cultures and results demonstrated LTLT-Ca cells exhibited increased migratory potential. Gene expression studies between LTLT-Ca mammospheres and LTLT-Ca adherent cells were performed, and our findings undoubtedly demonstrated that caveolin-associated genes were significantly downregulated. Reportedly, loss of caveolin 1 (CAV1) is found to be associated with poor patient outcomes. More specifically, the absence of CAV1 in breast cancer stroma is associated with poor clinical outcomes (34-36), including early tumor recurrence, lymph node metastasis, and tamoxifen resistance. Additionally, when CAV1 was silenced in stromal cells, it promoted tumor growth in breast cancer xenograft mouse models (37), suggesting that CAV1 functions as a tumor suppressor. This is a significant finding as CAV1 downregulation leads to the loss of E-cadherin and increased transcriptional activity of β-catenin, as well as enhanced tumor cell invasion (38). The loss of E-cadherin in LTLT-Ca mammospheres was expected as previous *in vivo* studies by our group have demonstrated that letrozole-resistant tumors express low levels of E-cadherin and high levels of N-cadherin (24). Herein, further loss of cell-cell adhesion, as indicated by the -6.44-fold decrease in E-cadherin expression, is associated with tumor progression, invasion, and metastasis, all of which are clinically relevant features of letrozole-resistant breast cancer. Consequently, decreased expression of genes that collectively promote cell adhesion (CAV1, CAV2, CDH1 and CTNNB1) enables cells to dissociate from the primary tumor and transition to a more mesenchymal phenotype. Ultimately, the cadherin/catenin complex is critical for epithelial integrity, while the consequences of β-catenin deletion have not been experimentally investigated, and the loss of E-cadherin-bound β-catenin correlates significantly with poor outcomes in breast cancer (39). While additional motility assays, like the invasion assay, were not performed, based on the LTLT-Ca mammosphere gene expression profile and migration assay results, it is likely the invasive behavior of the LTLT-Ca cells will follow a similar trend as the migratory behavior.

Furthermore, gene expression studies revealed the upregulation of two genes: six transmembrane epithelial antigen of prostate 1 (STEAP1) and tissue factor pathway inhibitor 2 (TFPI2). STEAP1 has roles in intercellular communication, serves as a channel or transporter, and is involved in cell adhesion (40). Although it has been previously reported that low STEAP1 expression is associated with a malignant phenotype and poor prognosis (41), the relationship between STEAP1 and breast cancer remains unclear. Moreover, previous reports have indicated conflicting roles for STEAP1 in breast cancer; however, our finding revealing increased STEAP1 expression in LTLT-Ca mammospheres supports the findings of Maia *et al* (42), which demonstrated that STEAP1 is overexpressed in the MCF-7 breast cancer cell line, human breast cancer epithelial cells, and rat mammary glands. Further studies are needed to confirm the contribution of STEAP1 in various subtypes of breast cancer. TFPI-2 was increased by 4.42-fold and is a serine protease inhibitor involved in preventing the release of matrix metalloproteinases. Additional reports have revealed that TFPI-2 suppresses breast cancer cell proliferation (43). As mammospheres are a surrogate reporter of CSCs, the increased TFPI-2 expression was not surprising as this cell subpopulation is relatively dormant and not highly proliferative.

In summary, we characterized letrozole-resistant mammospheres using the mammospheres formation assay, immunoblotting of cells and tumors, and gene expression arrays. Letrozole-resistant mammospheres were associated with the expression of $CD44^+/CD24^+$, increased stemness, invasive markers, and increased migration. Collectively, as letrozole resistance is more highly associated with CSCs, this may provide mechanistic insight into a new strategy to target the drug-resistant nature of AI-resistant breast cancer. Future studies may require analysis of letrozole sensitive mammospheres to pin-point the molecular pathways contributing to drug sensitivity within the cancer stem cell population which ultimately may reveal new targets to exploit for breast cancer patients.

Acknowledgements

The authors would like to thank Mrs. Tonya Bryant and Dr Boyada Tep from the College of Pharmacy and Pharmaceutical Sciences, Institute of Public Health, Florida A&M University, Tallahassee, FL, USA for assisting with the immunohistochemistry slides.

Funding

This work was supported in part by the National Institutes of Health (NIH; grant no. 1SC1GM126617). This publication was supported by funding from the Louisiana Cancer Research Consortium and the National Institutes of Health Research Centers at Minority Institutes (grant nos. 8G12MD007595 and U54MD007582) from the National Institute on Minority Health and Health Disparities. The contents are solely the responsibility of the authors and do not necessarily represent the official views of the Louisiana Cancer Research Consortium or the NIH.

Availability of data and materials

The datasets used and/or analyzed during the current study are available from the corresponding author on reasonable request.

Authors' contributions

SLT directed the project and conceived and designed the experiments. KMG, JRP, RRW and ID performed the experiments. KMG, JRP, RRW, AMD and ID contributed to data acquisition. AMD provided technical editing. JRP and KMG confirmed the authenticity of all the raw data. SLT, JRP, and KMG analyzed and interpreted the data. SLT, JRP and KMG wrote the manuscript. All authors read and approved the final manuscript.

Ethics approval and consent to participate

All animal experiments were approved by the Xavier University of Louisiana Institutional Animal Care and Use Committee (New Orleans, USA).

Patient consent for publication

Not applicable.

Competing interests

The authors declare that they have no competing interests.

References

1. Gilani RA, Kazi AA, Shah P, Schech AJ, Chumsri S, Sabnis G, Jaiswal AK and Brodie AH: The importance of her2 signaling in the tumor-initiating cell population in aromatase inhibitor-resistant breast cancer. Breast Cancer Res Treat 135: 681-692, 2012.
2. Brodie A, Jelovac D, Macedo L, Sabnis G, Tilghman S and Goloubeva O: Therapeutic observations in MCF-7 aromatase xenografts. Clin Cancer Res 11: 884s-888s, 2005.
3. Brodie A, Jelovac D, Sabnis G, Long B, Macedo L and Goloubeva O: Model systems: Mechanisms involved in the loss of sensitivity to letrozole. J Steroid Biochem Mol Biol 95: 41-48, 2005.
4. Jelovac D, Sabnis G, Long BJ, Macedo L, Goloubeva OG and Brodie AM: Activation of mitogen-activated protein kinase in xenografts and cells during prolonged treatment with aromatase inhibitor letrozole. Cancer Res 65: 5380-5389, 2005.
5. Sabnis G and Brodie A: Adaptive changes results in activation of alternate signaling pathways and resistance to aromatase inhibitor resistance. Mol Cell Endocrinol 340: 142-147, 2011.
6. Sabnis G, Schayowitz A, Goloubeva O, Macedo L and Brodie A: Trastuzumab reverses letrozole resistance and amplifies the sensitivity of breast cancer cells to estrogen. Cancer Res 69: 1416-1428, 2009.
7. Tilghman SL, Townley I, Zhong Q, Carriere PP, Zou J, Llopis SD, Preyan LC, Williams CC, Skripnikova E, Bratton MR, *et al*: Proteomic signatures of acquired letrozole resistance in breast cancer: Suppressed estrogen signaling and increased cell motility and invasiveness. Mol Cell Proteomics 12: 2440-2455, 2013.
8. Kalluri R and Weinberg RA: The basics of epithelial-mesenchymal transition. J Clin Invest 119: 1420-1428, 2009.
9. Tsai JH and Yang J: Epithelial-mesenchymal plasticity in carcinoma metastasis. Genes Dev 27: 2192-2206, 2013.
10. Gupta PB, Chaffer CL and Weinberg RA: Cancer stem cells: Mirage or reality? Nat Med 15: 1010-1012, 2009.
11. Mani SA, Guo W, Liao MJ, Eaton EN, Ayyanan A, Zhou AY, Brooks M, Reinhard F, Zhang CC, Shipitsin M, Campbell LL, Polyak K, Brisken C, Yang J and Weinberg RA: The epithelial-mesenchymal transition generates cells with properties of stem cells. Cell 133: 704-715, 2008.
12. Al-Hajj M and Clarke MF: Self-renewal and solid tumor stem cells. Oncogene 23: 7274-7282, 2004.
13. Al-Hajj M, Wicha MS, Benito-Hernandez A, Morrison SJ and Clarke MF: Prospective identification of tumorigenic breast cancer cells. Proc Natl Acad Sci USA 100: 3983-3988, 2003.
14. Armstrong AJ, Marengo MS, Oltean S, Kemeny G, Bitting RL, Turnbull JD, Herold CI, Marcom PK, George DJ and Garcia-Blanco MA: Circulating tumor cells from patients with advanced prostate and breast cancer display both epithelial and mesenchymal markers. Mol Cancer Res 9: 997-1007, 2011.
15. van der Horst G, Bos L and van der Pluijm G: Epithelial plasticity, cancer stem cells, and the tumor-supportive stroma in bladder carcinoma. Mol Cancer Res 10: 995-1009, 2012.
16. Weiswald LB, Bellet D and Dangles-Marie V: Spherical cancer models in tumor biology. Neoplasia 17: 1-15, 2015.
17. Serrano M: The ink4a/arf locus in murine tumorigenesis. Carcinogenesis 21: 865-869, 2000.
18. Cicalese A, Bonizzi G, Pasi CE, Faretta M, Ronzoni S, Giulini B, Brisken C, Minucci S, Di Fiore PP and Pelicci PG: The tumor suppressor p53 regulates polarity of self-renewing divisions in mammary stem cells. Cell 138: 1083-1095, 2009.
19. Dey D, Saxena M, Paranjape AN, Krishnan V, Giraddi R, Kumar MV, Mukherjee G and Rangarajan A: Phenotypic and functional characterization of human mammary stem/progenitor cells in long term culture. PLoS One 4: e5329, 2009.
20. Manuel Iglesias J, Beloqui I, Garcia-Garcia F, Leis O, Vazquez-Martin A, Eguiara A, Cufi S, Pavon A, Menendez JA, Dopazo J and Martin AG: Mammosphere formation in breast carcinoma cell lines depends upon expression of e-cadherin. PLoS One 8: e77281, 2013.
21. Gupta A, Mehta R, Alimirah F, Peng X, Murillo G, Wiehle R and Mehta RG: Efficacy and mechanism of action of proellex, an anti-progestin in aromatase overexpressing and letrozole resistant t47d breast cancer cells. J Steroid Biochem Mol Biol 133: 30-42, 2013.
22. Capes-Davis A, Reid YA, Kline MC, Storts DR, Strauss E, Dirks WG, Drexler HG, MacLeod RA, Sykes G, Kohara A, *et al*: Match criteria for human cell line authentication: Where do we draw the line? Int J Cancer 132: 2510-2519, 2013.
23. Johnson KP, Yearby LA, Stoute D, Burow ME, Rhodes LV, Gray M, Carriere P, Tilghman SL, McLachlan JA, Ochieng J, *et al*: In vitro and in vivo evaluation of novel anticancer agents in triple negative breast cancer models. J Health Care Poor Underserved 24 (Suppl 1): 104-111, 2013.
24. Carriere PP, Llopis SD, Naiki AC, Nguyen G, Phan T, Nguyen MM, Preyan LC, Yearby L, Pratt J, Burks H, *et al*: Glyceollin i reverses epithelial to mesenchymal transition in letrozole resistant breast cancer through zeb1. Int J Environ Res Public Health 13: ijerph13010010, 2016.
25. Livak KJ and Schmittgen TD: Analysis of relative gene expression data using real-time quantitative pcr and the 2(-delta delta c(t)) method. Methods 25: 402-408, 2001.
26. Pfaffl MW, Lange IG, Daxenberger A and Meyer HH: Tissue-specific expression pattern of estrogen receptors (ER): Quantification of ER alpha and ER beta mRNA with real-time RT-PCR. Acta Pathol Microbiol Scand Suppl 109: 345-355, 2001.
27. Creighton CJ, Li X, Landis M, Dixon JM, Neumeister VM, Sjolund A, Rimm DL, Wong H, Rodriguez A, Herschkowitz JI, *et al*: Residual breast cancers after conventional therapy display mesenchymal as well as tumor-initiating features. Proc Natl Acad Sci USA 106: 13820-13825, 2009.

28. Dontu G, Abdallah WM, Foley JM, Jackson KW, Clarke MF, Kawamura MJ and Wicha MS: In vitro propagation and transcriptional profiling of human mammary stem/progenitor cells. Genes Dev 17: 1253-1270, 2003.
29. Du L, Wang H, He L, Zhang J, Ni B, Wang X, Jin H, Cahuzac N, Mehrpour M, Lu Y and Chen Q: Cd44 is of functional importance for colorectal cancer stem cells. Clin Cancer Res 14: 6751-6760, 2008.
30. Ricardo S, Vieira AF, Gerhard R, Leitao D, Pinto R, Cameselle-Teijeiro JF, Milanezi F, Schmitt F and Paredes J: Breast cancer stem cell markers cd44, cd24 and aldh1: Expression distribution within intrinsic molecular subtype. J Clin Pathol 64: 937-946, 2011.
31. Li W, Ma H, Zhang J, Zhu L, Wang C and Yang Y: Unraveling the roles of cd44/cd24 and aldh1 as cancer stem cell markers in tumorigenesis and metastasis. Sci Rep 7: 13856, 2017.
32. Li W, Ma H, Zhang J, Zhu L, Wang C and Yang Y: Author correction: Unraveling the roles of cd44/cd24 and aldh1 as cancer stem cell markers in tumorigenesis and metastasis. Sci Rep 8: 4276, 2018.
33. Oliveras-Ferraros C, Vazquez-Martin A, Martin-Castillo B, Cufí S, Del Barco S, Lopez-Bonet E, Brunet J and Menendez JA: Dynamic emergence of the mesenchymal cd44(pos)cd24(neg/low) phenotype in her2-gene amplified breast cancer cells with de novo resistance to trastuzumab (herceptin). Biochem Biophys Res Commun 397: 27-33, 2010.
34. Simpkins SA, Hanby AM, Holliday DL and Speirs V: Clinical and functional significance of loss of caveolin-1 expression in breast cancer-associated fibroblasts. J Pathol 227: 490-498, 2012.
35. Sloan EK, Ciocca DR, Pouliot N, Natoli A, Restall C, Henderson MA, Fanelli MA, Cuello-Carrión FD, Gago FE and Anderson RL: Stromal cell expression of caveolin-1 predicts outcome in breast cancer. Am J Pathol 174: 2035-2043, 2009.
36. Witkiewicz AK, Dasgupta A, Sotgia F, Mercier I, Pestell RG, Sabel M, Kleer CG, Brody JR and Lisanti MP: An absence of stromal caveolin-1 expression predicts early tumor recurrence and poor clinical outcome in human breast cancers. Am J Pathol 174: 2023-2034, 2009.
37. Trimmer C, Sotgia F, Whitaker-Menezes D, Balliet RM, Eaton G, Martinez-Outschoorn UE, Pavlides S, Howell A, Iozzo RV, Pestell RG, *et al*: Caveolin-1 and mitochondrial sod2 (mnsod) function as tumor suppressors in the stromal microenvironment: A new genetically tractable model for human cancer associated fibroblasts. Cancer Biol Ther 11: 383-394, 2011.
38. Lu Z, Ghosh S, Wang Z and Hunter T: Downregulation of caveolin-1 function by egf leads to the loss of e-cadherin, increased transcriptional activity of beta-catenin, and enhanced tumor cell invasion. Cancer Cell 4: 499-515, 2003.
39. Dolled-Filhart M, McCabe A, Giltnane J, Cregger M, Camp RL and Rimm DL: Quantitative in situ analysis of beta-catenin expression in breast cancer shows decreased expression is associated with poor outcome. Cancer Res 66: 5487-5494, 2006.
40. Gomes IM, Maia CJ and Santos CR: Steap proteins: From structure to applications in cancer therapy. Mol Cancer Res 10: 573-587, 2012.
41. Xie J, Yang Y, Sun J, Jiao Z, Zhang H and Chen J: Steap1 inhibits breast cancer metastasis and is associated with epithelial-mesenchymal transition procession. Clin Breast Cancer 19: e195-e207, 2019.
42. Maia CJ, Socorro S, Schmitt F and Santos CR: Steap1 is over-expressed in breast cancer and down-regulated by 17beta-estradiol in mcf-7 cells and in the rat mammary gland. Endocrine 34: 108-116, 2008.
43. Wang G, Huang W, Li W, Chen S, Chen W, Zhou Y, Peng P and Gu W: Tfpi-2 suppresses breast cancer cell proliferation and invasion through regulation of erk signaling and interaction with actinin-4 and myosin-9. Sci Rep 8: 14402, 2018.